

This is an Open Access document downloaded from ORCA, Cardiff University's institutional repository:<https://orca.cardiff.ac.uk/id/eprint/89580/>

This is the author's version of a work that was submitted to / accepted for publication.

Citation for final published version:

Ng, Wai Siene, Legg, Phil, Avadhanam, Venkat, Aye, Kyaw, Evans, Steffan H. P., North, Rachel Valerie, Marshall, Andrew D., Rosin, Paul L. and Morgan, James Edwards 2016. Automated registration of multimodal optic disc images: clinical assessment of alignment accuracy. *Journal of Glaucoma* 25 (4), pp. 397-402.
10.1097/IJG.0000000000000252

Publishers page: <http://dx.doi.org/10.1097/IJG.0000000000000252>

Please note:

Changes made as a result of publishing processes such as copy-editing, formatting and page numbers may not be reflected in this version. For the definitive version of this publication, please refer to the published source. You are advised to consult the publisher's version if you wish to cite this paper.

This version is being made available in accordance with publisher policies. See <http://orca.cf.ac.uk/policies.html> for usage policies. Copyright and moral rights for publications made available in ORCA are retained by the copyright holders.



AUTOMATED REGISTRATION OF MULTIMODAL OPTIC DISC IMAGES: CLINICAL ASSESSMENT OF ALIGNMENT ACCURACY

Wai Siene Ng FRCOphth¹, Venkat Avadhanam FRCOphth¹; Phil Legg PhD¹; Kyaw Aye², Steffan Huw Prosser Evans MBBCh³, Rachel Valerie North PhD³, Andrew David Marshall PhD³, Paul Rosin PhD², James Edwards Morgan FRCOphth^{1,2}.

WS Ng, V Avadhanam, K Aye: University Hospital Wales, Cardiff CF14 4XW, Wales, UK
RV North, JE Morgan: Cardiff Centre for Vision Sciences, Cardiff University, Maindy Road CF24 4HQ, Wales, UK,
PA Legg, D Marshall, PL Rosin: School of Computer Sciences and Informatics, Cardiff University CF24 3AA, Wales, UK.
SHP Evans: Royal Glamorgan Hospital, Llantrisant, CF72 8XR, Wales UK.

ABSTRACT

Aims:

To determine the accuracy of automated alignment algorithms for the registration of optic disc images obtained by two different modalities: fundus photography and scanning laser tomography.

Methods:

Images obtained with the Heidelberg Retina Tomograph II and paired photographic optic disc images of 135 eyes were analysed. Three state-of-the-art automated registration techniques Regional Mutual Information (RMI), rigid Feature Neighbourhood Mutual Information [FNMI] and non-rigid FNMI (NRFNMI) were used to align these image pairs. Alignment of each composite picture was assessed on a five point grading scale: 'Fail' (no alignment of vessels with no vessel contact), 'Weak' (vessels have slight contact), 'Good' (vessels with less than 50% contact), 'Very Good' (vessels with more than 50% contact) and 'Excellent' (complete alignment). Custom software generated an image mosaic in which the modalities were interleaved as a series of alternate 5 × 5 pixel blocks. These were graded independently by three clinically experienced observers.

Results:

810 image pairs were assessed. All three registration techniques achieved a score of 'Good' or better in more than 95% of the image sets. NRFNMI had the highest percentage of 'Excellent' (mean: 99.6% range: 95.2-99.6%), followed by RMI (mean: 81.6% range: 86.3-78.5%) and FNMI (mean: 73.1% range: 85.2-54.4%).

Conclusion:

Automated registration of optic disc images by different modalities is a feasible option for clinical application. All three methods provided useful levels of alignment but the NRFNMI technique consistently outperformed the others and is recommended as a practical approach to the automated registration of multimodal disc images.

KEYWORDS:

Multimodal registration, Glaucoma, Imaging, Optic nerve, Diagnostic tests/Investigation

INTRODUCTION

The digitisation of fundal imaging has transformed the clinical assessment of retinal disease. While the digitisation of retinal photography has been a major step forward, some of the most exciting developments have come from the introduction of laser based imaging modalities which have provided clinically relevant information on retinal structure. Scanning laser ophthalmoscopy was first to generate high resolution topographic plots of the retinal surface[1-3]. More recently, optical coherence tomography has entered routine use for the quantitative assessment of retinal structure at near cellular resolutions[4-6]. Other modalities such as scanning laser polarimetry have provided complimentary information related to the thickness of the retinal nerve fibre layer[7-10]

In spite of these advances, the clinical assessment of retinal disease still relies on indirect ophthalmoscopy and in digital form, fundus photography. Clinicians are therefore presented with multimodal views of the retina for which the derivation of a combined image dataset can be problematic. The registration of images obtained by different modalities would appear to offer considerable advantages[11] and is routinely used in other areas of clinical imaging such as CT-MRI. For example, photographic views of the optic disc can provide clear views of the optic disc margin which are important for the derivation of optic disc parameters in the diagnosis of glaucoma. Similarly, retinal drusen may be more apparent in photographic than in coherence based views[12,13]. The use of a common photographic platform for image registration would also be beneficial for the follow-up of patients. There is, therefore, a recognised need for efficient and accurate image registration to combine information from images acquired using different modalities.

Several investigators have reported methods for the registration of images[1,14]. Best results are generated when the observer selects retinal landmarks (fiducial points) that are on the basis of known anatomical features, judged to arise from the same points in the retina[1,3]. Unfortunately, fully automated registration can result in lower levels of alignment accuracy, which might limit use of these algorithms in the clinical setting particularly when image clarity might be an issue.

Since the automated registration of retinal images generated by differing modalities would facilitate clinical implementation, we have explored novel methods for the automated registration of these images. As a test dataset that is representative of the types of images to be registered, we have taken extended focus images derived from the Heidelberg Retina Tomography II (HRT-II) and aligned these to digital optic disc photographs of the same field of view. Based on preliminary work we selected three algorithms for the automated alignment of the image pairs. All were based on a mutual information (MI) approach[4,6] which is widely used to register images of biological structures of different modalities. It is an entropy based measure that maximises the interdependence of the two images under consideration.

While mutual information methods have been used successfully we hypothesised that the accuracy of alignment could be further improved by the inclusion of the spatial distribution of neighbouring pixels and intensity mapping (Feature Neighbourhood Mutual Information: FNMI). FNMI algorithms were applied in two forms. In the first, the images maintained their respective spatial arrangements and were not deformed (rigid FNMI). We then used a recently developed non-rigid FNMI method (NRFNMI) in which registration was enhanced locally using a local mutual information window. We report the performance of both the rigid and non-rigid FNMI algorithms as well as the widely used MI approach in the registration of optic disc photographs with HRT scans.

MATERIALS AND METHODS

Registration was performed on 135 matching image pairs of colour fundus photographs and scanning laser ophthalmoscopy (SLO) images centred on the optic disc. The images were obtained during the course of routine glaucoma care at the University Hospital of Wales with all patients providing written consent for images to be used for subsequent analysis and publication. The data

set of images included a range of normal, early glaucomatous and advanced glaucoma subjects. Fundus photographs were acquired using a TOPCON TRC50-EX with a Nikon digital camera providing images with a resolution of 3008 × 1960 pixels (24 bits per pixel). SLO images were captured with a HRT-II (Heidelberg Retina Engineering). The field of view for the SLO images subtended at 15 × 15 degrees and comprised of 384 × 384 pixels. Since the HRT-II takes images at 32 focal depths, the intensity value at each pixel location was summed to generate a single intensity values in a single image (8 bits per pixel). Images were viewed with a bitmap palette that approximated the colour of the retina.

For the purposes of grading the quality of the alignment of these image pairs, they were presented as a static image in which the registration results were presented using a mosaic formation (5 × 5 grid of pixels for the area covered by the HRT image) to show the overlap between the two images (see Figure 1c). In the first set, the pixel block at X[0] Y[0] represented the HRT image and in the second set, this pixel block started with the fundus photograph image. Each image was therefore graded twice but with alternating areas of each image used for comparison thereby generating 270 images to test each algorithm. The following registration techniques were evaluated: FNMI, NRFNMI and RMI. The registration time was reduced by presenting the fundus images as a 564 × 367 pixel array and the HRT image as a 288 × 288 pixel array. The fundus photograph was used as the reference image with the location of the HRT image adjusted to provide the registration.

Image grading

The grading system is illustrated in Figure 1. The alignment was deemed as 'Fail' if vessels with the same point of origin had no point of contact. Alignment was 'Weak' if the vessels contacted but overlapped less than 20%. Above this (up to 50% overlap) the alignment was judged to be 'Good'. With greater than 50% of overlap, the alignment was judged to be 'Very Good'. When the vessels showed complete alignment (no vessel border discontinuity) the overall quality of the alignment was judged as 'Excellent'. An example of an image pair with 'Very Good' alignment is shown in Figure 1c.

Image alignment techniques

RMI (Regional Mutual information) extends the standard MI method by incorporating at each pixel the additional intensities of all pixels within a fixed size neighbourhood. To avoid the enormous joint histograms that would arise when using the standard MI approach, the neighbourhood was described by its covariance matrix, from which it is possible to efficiently compute MI[15]. Secondly, a registration search for transformation space was performed by incorporating a multi-resolution image pyramid. The translational search was optimised using the Nelder-Mead simplex algorithm[10].

As with RMI, rigid FNMI alignment[7,9] computes a MI score that incorporates more information than just individual pixels from the image pair. This was achieved by including the gradient magnitudes of each image that were calculated at multiple spatial scales to detect structural and spatial aspects of the images.

The aim of the NRFNMI is to refine the results of rigid FNMI by allowing for some deformation of the image. Within the area of interest, the two images to be registered were subdivided into a set of 4 × 4 windows. The centre points from these 16 windows defined our initial control points for performing the non-rigid deformation. Each window was subdivided into another set of 4 × 4 windows, and a normalised mutual information score computed for each of these smaller windows. The overall MI score was given by the sum of individual smaller window MI scores. The translational search of each subwindow was limited to a 3 pixel-radius in the central 4 windows and a 5 pixel-radius in the outer 12 windows to prevent window misplacement. Finally, deformation of the SLO image was performed by taking the central points of the large 16 windows as controls. A thin-plate spline warp algorithm was applied to determine the amount of deformation.

Statistical Analysis

Results between the three registration methods were analysed by chi-square test (P-value less than 0.05). Intraclass correlation coefficients (ICC) between the three assessors for the three methods were calculated using a two-way mixed model. Statistical analysis was carried out with IBM SPSS Statistics version 20 software.

RESULTS

All images were judged to be of suitable quality for the purposes of grading. We did not observe any systematic bias in images for regions that were consistently misaligned. An image grade was assigned on the basis of an area of misalignment within the region of interest; as shown in Figure 1c, the overall level of grading would be 'Very Good' due to vessel border misalignments seen on the inferotemporal arcade vessels. The distributions of alignment scores for the three observers are shown for the three methods of registration in figures 2-4. The proportion of alignment graded as failing was less than 1% (mean value across observers) for all registration methods. All three techniques had more than 96% of the images marked as "Good" or better by all the three independent observers. The proportion of alignments scoring 'Excellent' was highest for the NRFNMI at 96.8% (range 99.6 - 95.2%); higher than FNMI* ($p=0.007$) and RMI ($p=0.254$). This was followed by RMI at 81.6% (range 86.3 - 78.5%) and FNMI at 73.1% (range 85.2 - 54.5%) [see Figure 5]. NRFNMI also had the highest percentage of "Good" or better grading comprising 99.8% of its total score. ICC showed positive agreement across all three assessors for all registration methods, ranging from 0.475 to 0.306 for FNMI, 0.456 to 0.142 for RMI and 0.401 to 0.140 for NRFNMI.

DISCUSSION

Ophthalmology is increasingly reliant on the integration of digital information from a range of modalities and devices. In the management of glaucoma, these device confer the greatest clinical power when used in combination[2,16-18]. Further diagnostic accuracy is also possible when consideration is given to the registration of visual field test locations and retinal structure[19]. Our study advances this by demonstrating the feasibility of registering retinal image datasets from two commonly used imaging modalities. The NRFNMI algorithm generated 'Excellent' levels of alignment in 96% of cases across all observers which is likely to be sufficient for translation to clinical practice. Importantly, these alignments were fully automated and did not require users to mark fiducial points to initiate the process.

Multimodal alignment technologies address an important need in ophthalmology to develop a common platform for the interrogation of retinal images. Fundus photographs remain the mainstay for the assessment of retinal diseases that may outlast the development cycle of many proprietary imaging technologies. Automated multimodal registration can provide complimentary views for the demarcation of regions of interest (e.g. demarcation of optic disc boundaries) which can be problematic in scanning laser images. In the interpretation of scanning laser tomographs, disc photographs can improve the demarcation of the optic disc margin whether this is undertaken by manual or automated methods[20]. The detection of other optic disc features indicative of disease such as retinal nerve fibre layer haemorrhages is improved with the inclusion of fundus photographs [5,21]

Our data confirm the importance of including local spatial information in the design of a retinal image alignment algorithm. The reflectivity distribution needs to be taken into consideration in a fundus and tomographic image. For example, the neuroretinal rim, which overlies the highly reflective lamina cribrosa corresponds to a region of high reflectivity. By contrast, the signal in a confocal image is low since the angle between the incidence laser beam and the retinal surface undergoes considerable changes at the margin of the optic disc resulting in light scatter [8,22]. In view of these considerations, the relatively lower score with the MI method is not surprising since it

uses pixel intensities rather than extracting structural features between images. Only individual pixel intensities are considered in this method but no spatial information is taken into account. Although MI is widely used in the field of medicine for registering images of different modalities, improvements to MI have been proposed. For example, with gradient MI, the standard MI is computed and is then multiplied by a gradient term[23]. A higher order MI proposed by Rueckert calculates entropy for intensity pairs rather than individual intensities [24].

All registration algorithms are vulnerable to the effects of local maxima in the registration surface, which can adversely affect search optimisation. Inclusion of the radius of the neighbourhood pixels improved the accuracy of registration with RMI, but also increased the matrix size and computational time. FNMI, a novel similarity measure technique developed by Legg [7,11,9,12,13] incorporates multi-scale feature derivatives along with spatial neighbourhood knowledge into the MI framework. The FNMI technique is advantageous in that excellent registration is provided for even blurred images, a drawback which often arises in clinical practice in the presence of cataract, high degrees of astigmatism or movement.

Although rigid FNMI provides accurate registration for most of the image pairs, subtle misalignments were apparent in certain sets. Differences in the acquisition techniques of SLO and fundus photography coupled with the alterations in eye position during image acquisition can lead to subtle elastic deformations in the images that will become manifest during rigid registration. Kubecka and Jan recommended a generalised elastic registration for the registration of fundus and SLO images as there can be some deformation between the two images [1,14].

In summary, NRFNMI based alignment is a novel time-efficient method that requires a fraction of the data need for RMI based alignment and delivers excellent registration accuracy. Further studies are required to evaluate the clinical validity of this technique for registration of other image modalities such as stereophotography and OCT. We anticipate that these algorithms will be suited to the alignment of same modality images and therefore for the detection of change in images taken over time, an essential paradigm for clinical practice.

REFERENCES

1. Chrástek R, Skokan M, Kubecka L et al. Multimodal retinal image registration for optic disk segmentation. *Methods Inf Med.* 2004;43(4):336–42.
2. Kamal D, Garway-Heath D, Hitchings R, Fitzke F. Use of sequential Heidelberg retina tomograph images to identify changes at the optic disc in ocular hypertensive patients at risk of developing glaucoma. *Br J Ophthalmol.* 2000;84(9):993-8.
3. Kolar R, Kubecka L, Jan J. Registration and fusion of the autofluorescent and infrared retinal images. *Int J Biomed Imaging.* 2008;2008:513478.
4. Viola PA, Wells WM. Alignment by maximization of mutual information. In: Proc 5th int conf on computer vision (Boston). *IEEE.* 1995:1523.
5. Drexler W, Fujimoto JG. State-of-the-art retinal optical coherence tomography. *Prog Retin Eye Res.* 2008;27(1):45-88.
6. Collignon A, Maes F, Delaere D et al. Automated multimodality image registration based on information theory. In: Bizais Y, Barillot C, Di Paola R, eds. *Information processing in medical imaging (Brest). Dordrecht (the Netherlands): Kluwer Academic.* 1995:263274.
7. Legg PA, Rosin PL, Marshall D, Morgan JE. Incorporating neighbourhood feature derivatives with Mutual Information to improve accuracy of multi-modal image registration. *Proc. Image Understanding and Analysis* 2008:39-43.
8. Boehm MD, Nedrud C, Greenfield DS, Chen PP. Scanning laser polarimetry and detection of progression after optic disc hemorrhage in patients with glaucoma. *Arch Ophthalmol.* 2003;121(2):189–94.
9. Legg PA, Rosin PL, Marshall D, Morgan JE. A robust solution to multi-modal image registration by combining mutual information with multi-scale derivatives. *Med Image Comput and Comput Assisted Interv.* 2009;12(Pt1):616-23.
10. Lagarias JC, Reeds JA, Wright MH, Wright P. Convergence properties of the Nelder-Mead simplex method in low dimensions. *SIAM J of Optim.* 1998;9(1):112–147.
11. Bernardes R, Lobo C, Cunha-Vaz JG. Multimodal macula mapping: a new approach to study diseases of the macula. *Surv Ophthalmol.* 2002;47(6):580–9.
12. Sohrab MA, Smith RT, Salehi-Had H, Sadda SR, Fawzi AA. Image registration and multimodal imaging of reticular pseudodrusen. *Invest Ophthalmol Vis Sci.* 2011;52(8):5743–8.
13. Forte R, Querques G, Querques L et al. Multimodal imaging of dry age-related macular degeneration. *Acta Ophthalmol.* 2012;90(4):e281–7.
14. Kubecka L, Jan J. Registration of bimodal retinal images - improving modifications. *Conf Proc IEEE Eng Med Biol Soc.* 2004;3:1695–8.
15. Russakoff DB, Tomasi C, Rohlifing T, Maurer CR. Image similarity using mutual information of regions. *ECCV* 2004;3:596–607.
16. Sanchez-Galeana C, Bowd C, Blumenthal EZ. Using optical imaging summary data to detect glaucoma. *Ophthalmol.* 2001;108(10):1812-8.

17. Reus NJ, de Graaf M, Lemij HG. Accuracy of GDx VCC, HRT I, and clinical assessment of stereoscopic optic nerve head photographs for diagnosing glaucoma. *Br J Ophthalmol*. 2007;91(3):313–8.
18. Greenfield DS, Weinreb RN. Role of optic nerve imaging in glaucoma clinical practice and clinical trials. *Am J Ophthalmol*. 2008;145(4):598–603.
19. Asaoka R, Russell RA, Malik R, Crabb DP, Garway-Heath DF. A novel distribution of visual field test points to improve the correlation between structure-function measurements. *Invest Ophthalmol Vis Sci*. 2012;53(13):8396–404.
20. Iester M, Mikelberg FS, Courtright P et al. Interobserver variability of optic disk variables measured by confocal scanning laser tomography. *Am J Ophthalmol*. 2001;132(1):57–62.
21. Budde WM, Mardin CY, Jonas JB. Glaucomatous optic disc hemorrhages on confocal scanning laser tomographic images. *J Glaucoma*. 2003;12(6):470–4.
22. Bartsch DU, Freeman WR. Axial intensity distribution analysis of the human retina with a confocal scanning laser tomograph. *Exp Eye Res*. 1994;58(2):161–73.
23. Pluim J, Maintz JA, Viergever MA. Interpolation artefacts in mutual information-based image registration. *Comput Vis Image Und*. 2000;77:211-232.
24. Rueckert D, Clarkson M, Hill D, Hawkes D. Non-rigid registration using higher-order mutual information. In: *Proc. SPIE Medical Imaging 2000: Image Processing*, San Diego, CA. 2000:438–447.
25. Beijing C, JunLi L, Gang C. Study of medical image registration based on second-order mutual information. *IEEE International Conference on Multimedia and Expo*. 2007;956–959.

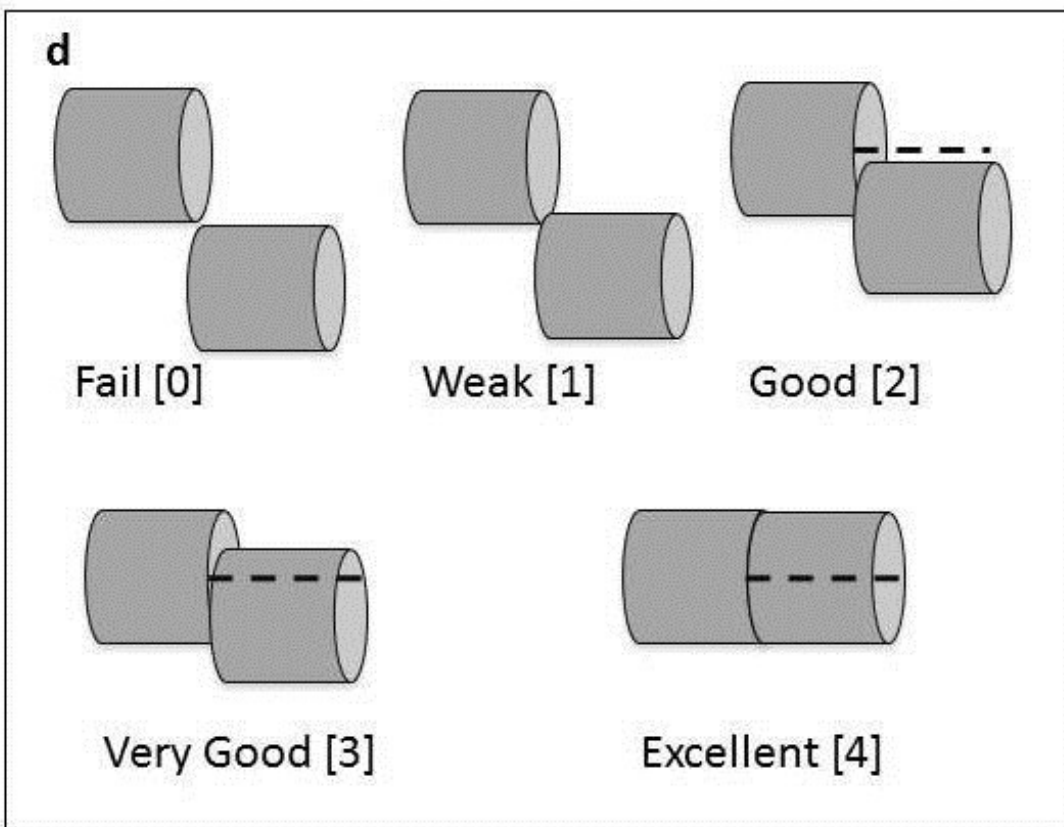
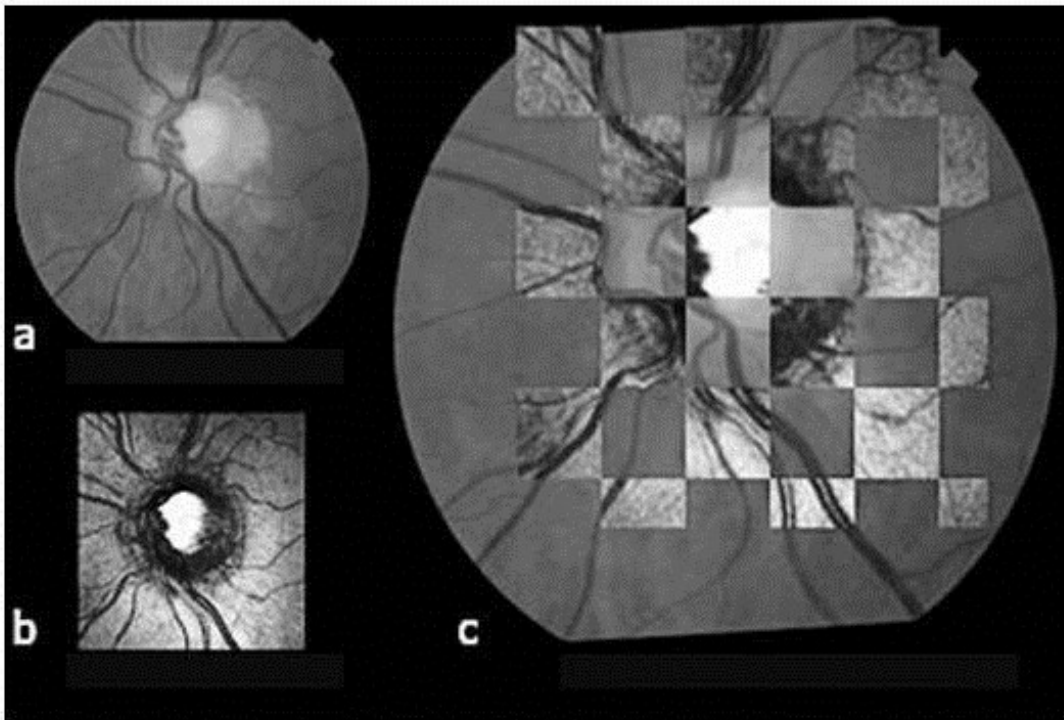


Figure 1. a: Fundus photograph of optic nerve head, b: Corresponding scanning laser ophthalmoscopy image of the same optic nerve head, c: Chequer-board arrangement used to grade alignment. The chequer-board pattern was counter phased so that each image pair was assessed on the base of two images, d: Illustration of alignment scores. “Fail”[0] = no point of contact, “Weak”[1] = vessels contacted but overlap less than 20%, “Good”[2] = up to 50% vessel overlap, “Very Good” [3] = greater than 50% vessel overlap, “Excellent”[4] = complete vessel alignment.

Feature Neighbourhood Mutual Information Registration

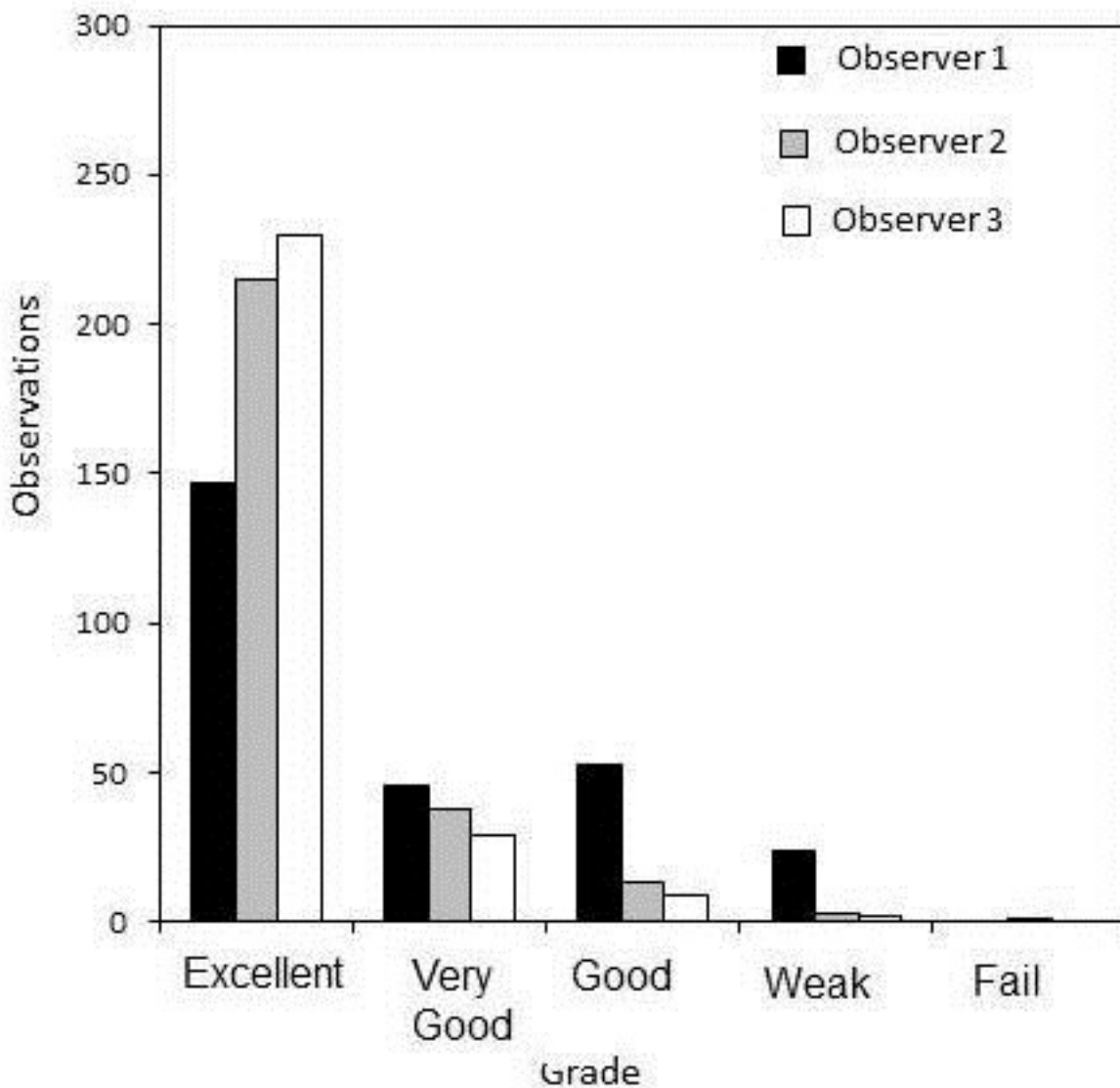


Figure 2. Histogram of alignment scores from the three observers for the Feature Neighbourhood Mutual Information (FNMI) registration method.

Regional Mutual Information Registration

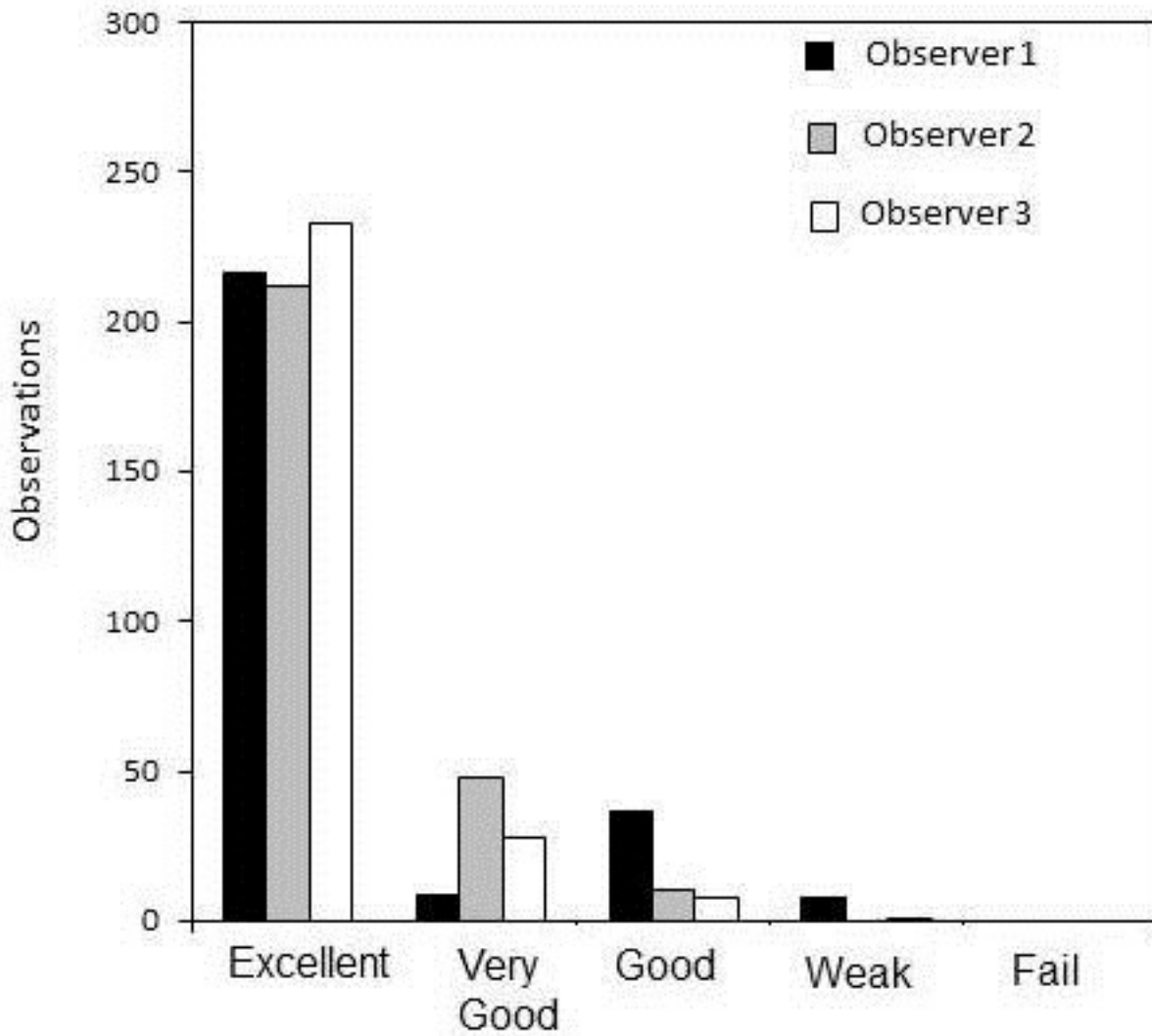


Figure 3. Histogram of alignment scores from the three observers for the Regional Mutual Information (RMI) registration method.

Non rigid FNMI registration

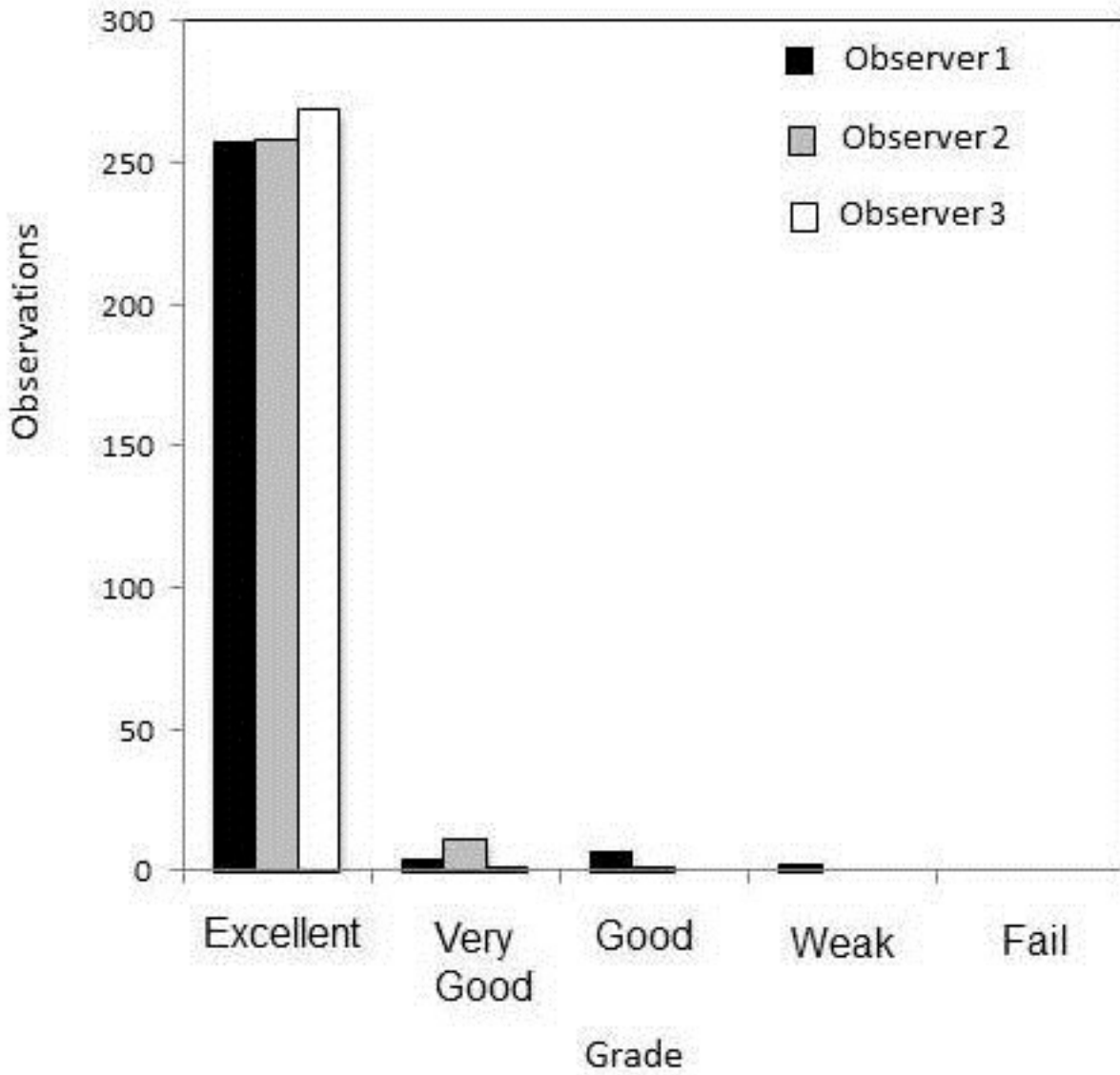


Figure 4. Histogram of alignment scores from the three observers for the Non-Rigid Feature Neighbourhood Mutual Information (NRFMI) registration method.

Comparative alignment method accuracy

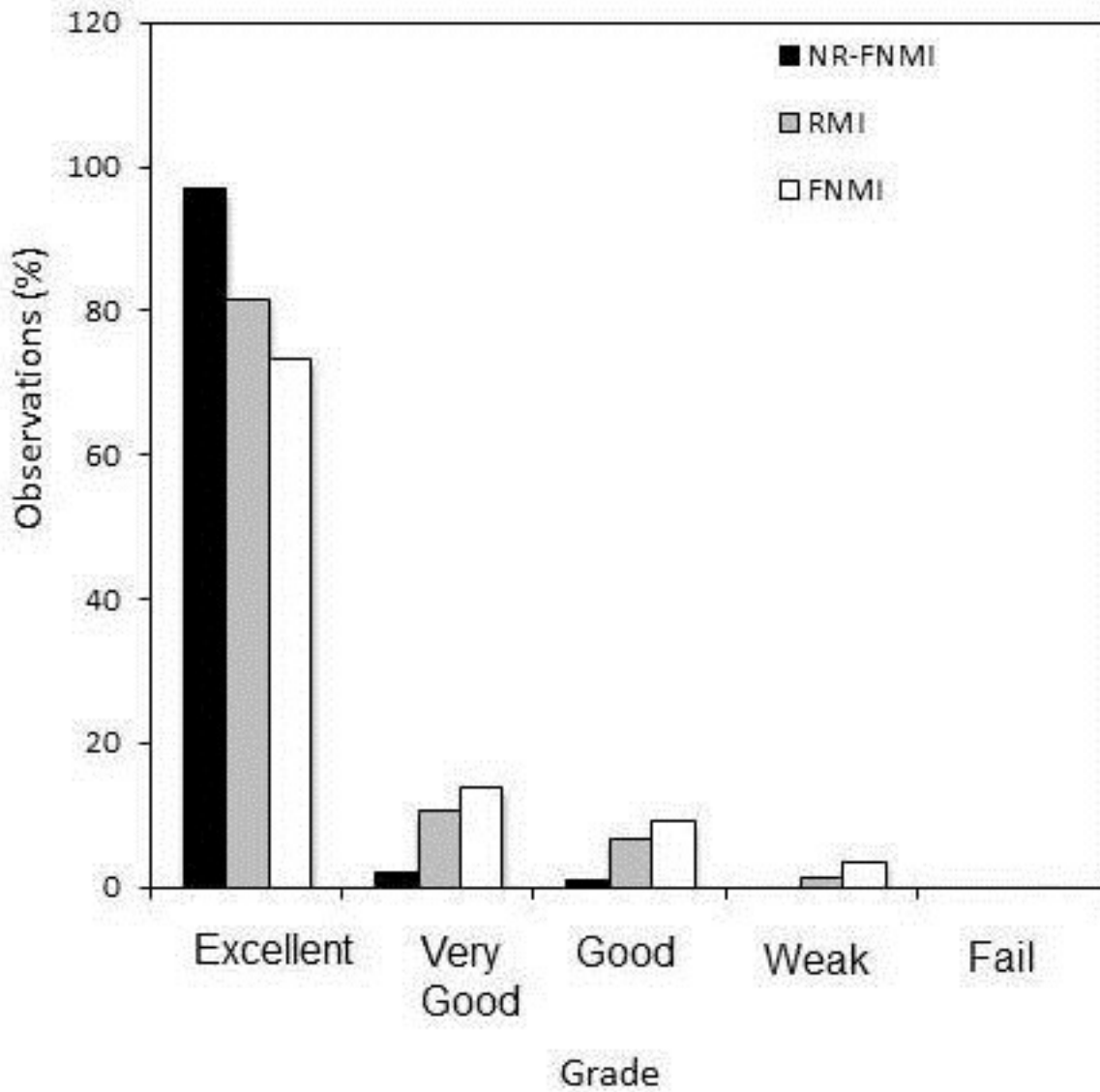


Figure 5. Histogram of comparative alignment accuracy scores between rigid Feature Neighbourhood Mutual Information (FNMI), Regional Mutual Information (RMI) and Non-Rigid Feature Neighbourhood Mutual Information (NRFNMI) registration methods.